

Design and Validation of the First Family of Photo-Activatable Ligands for Melatonin Receptors

Gloria Somalo-Barranco, Carme Serra, David Lyons, Hugh D. Piggins, Ralf Jockers,* and Amadeu Llebaria*

Cite This: *J. Med. Chem.* 2022, 65, 11229–11240

Read Online

ACCESS |



Metrics & More

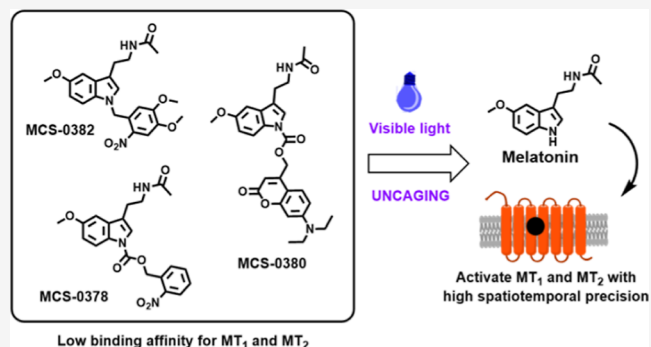


Article Recommendations



Supporting Information

ABSTRACT: Melatonin is a neurohormone released in a circadian manner with peak levels at night. Melatonin mediates its effects mainly through G protein-coupled MT₁ and MT₂ receptors. Drugs acting on melatonin receptors are indicated for circadian rhythm- and sleep-related disorders. Tools to study the activation of these receptors with high temporal resolution are lacking. Here, we synthesized a family of light-activatable caged compounds by attaching *o*-nitrobenzyl (*o*-NB) or coumarin photocleavable groups to melatonin indolic nitrogen. All caged compounds showed the expected decrease in binding affinity for MT₁ and MT₂. The *o*-NB derivative MCS-0382 showed the best uncaging and biological properties, with 250-fold increase in affinity and potency upon illumination. Generation of melatonin from MCS-0382 was further demonstrated by its ability to modulate the excitation of SCN neurons in rat brain slices. MCS-0382 is available to study melatonin effects in a temporally controlled manner in cellular and physiological settings.



INTRODUCTION

Melatonin (5-methoxy-*N*-acetyltryptamine) is a hormone that is predominantly secreted by the pineal gland, following a circadian rhythm with high levels at night.¹ Melatonin regulates many physiological functions in the body including the regulation of biological rhythms, sleep, pain, retinal, neuronal, and immune functions.² These effects are mainly mediated through the activation of two members of the G protein-coupled receptor (GPCR) family, MT₁ and MT₂ receptors, which preferentially couple to Gi/o proteins.³ Commercialized drugs targeting melatonin receptors are used to ameliorate sleep onset, depressive disorders, and dysfunctions related to the circadian rhythms.² Future possible therapeutic applications include the treatment of pain, inflammation, immune system disorders, and metabolic and neurodegenerative diseases.²

Light is now increasingly recognized as an ideal external control element to modulate physiological systems with a high spatiotemporal precision associated to a low toxicity and high safety.⁴ In this context, photopharmacology is presented as a discipline based on the development of molecular probes whose biological activity can be regulated by light. Light can be adjusted to most cellular processes, not interfering or damaging the living system, and it can be manipulated remotely. Furthermore, the extent of its effect can be precisely regulated through the adjustment of the wavelength and intensity of the light.⁵ Two of the most widely used molecular approaches that

incorporate light to control biological processes are photo-switches and caged compounds, where the main difference is the reversibility of the process upon the application of light.⁶ In biological chemistry and pharmacology, a caged compound is a light-sensitive probe that is obtained by attaching covalently a photo-cleavable group to a bioactive molecule. This modification is designed to render the new ligand inactive to the target receptor. Under suitable light conditions, an irreversible photolytic reaction is triggered in the caged molecule, which releases specifically the active molecule at the action site.⁷

Light-dependent control of receptor activity has been already achieved for several GPCRs,^{8,9} contributing to a better understanding of receptor function. In particular, light-controlled release of the active ligand upon uncaging provides valuable insights about receptor-induced signaling or binding kinetics.¹⁰ In contrast to conventional pharmacology, in photopharmacology, light induces an abrupt change in the concentration of the active molecule at the action site, providing a high spatiotemporal resolution of the process of

Received: May 6, 2022

Published: August 5, 2022



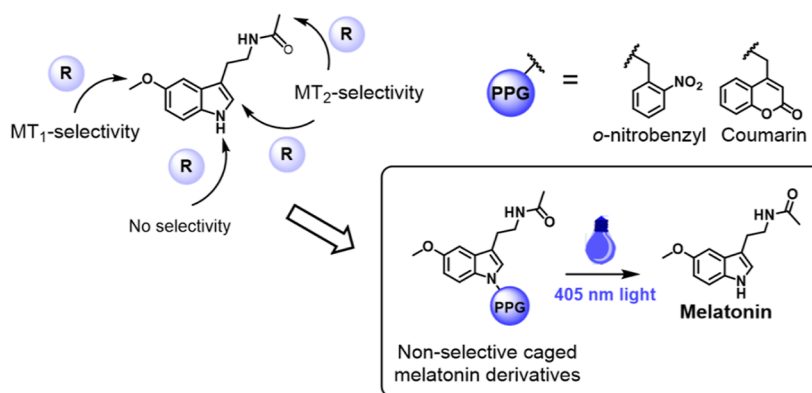
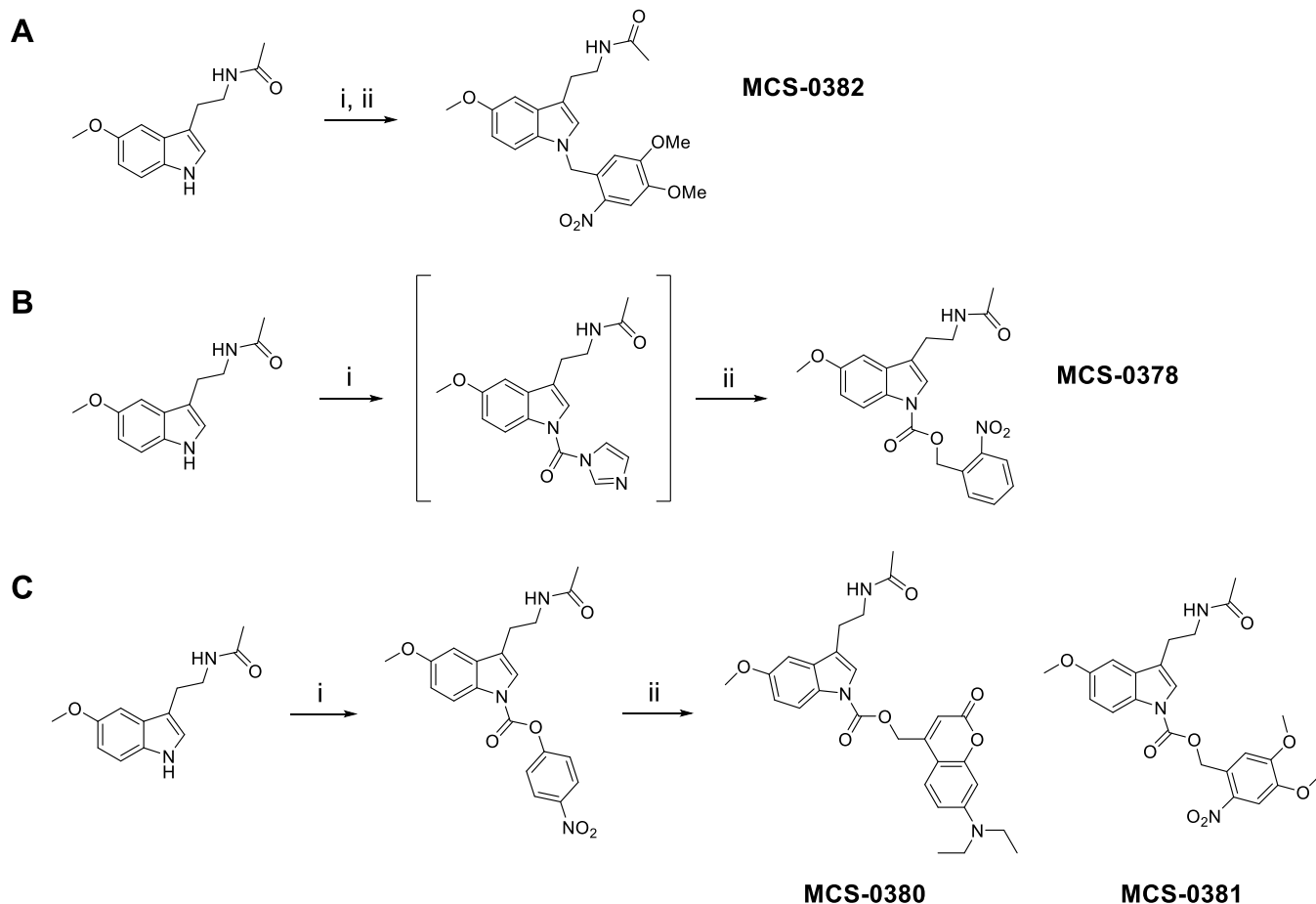


Figure 1. Chemical design of the caged melatonin derivatives presented here. Following the caging strategy, a photoprotective group is attached at the N1-position, achieving a decrease on binding affinity for melatonin receptors, without selectivity for MT₁ or MT₂. The new light-sensitive molecules release active melatonin under suitable light conditions.

Scheme 1. Chemical Synthesis of Compounds MCS-0378, MCS-0380, MCS-0381, and MCS-0382



Reagents and conditions: (A) (i) NaH, DMF, 0 °C, 30 min, (ii) DMNB-Br, DMF, -40 °C, 15 h, 35%; (B) (i) CDI, DMAP, ACN, 40 °C, 30 min, (ii) *o*-NB alcohol, ACN, reflux, 2 days, 15%; (C) reagents and conditions: (i) 4-nitrophenyl chloroformate, TEA, DMAP, ACN, reflux, 12h, 49%, (ii) DEAC-OH or DMNB-OH, DMAP, ACN, reflux, 3 or 6 days, 53 and 26% for MCS-0380 and MCS-0381, respectively. Details on the synthesis of DEAC-OH are provided in the [Supporting Information](#) (scheme S1).

interest.¹¹ Photopharmacology has never been applied to melatonin receptors but would be very useful for precise spatial-temporal activation of melatonin receptors *in vitro* and *in vivo*. Using light to control melatonin receptor activation will be a powerful new pharmacological tool to study the function of these receptors. Light-induced activation of melatonin receptors at specific locations (tissues and brain

regions) appears a promising approach to study its effects in experimental biology and pharmacology. Melatonin is known to regulate the sleep/wake cycle and to affect sleep stages, but the actual participation of the different brain region(s) expressing melatonin receptors and known to be involved in sleep regulation (i.e., reticular thalamus, the lateral hypothalamus, and the ventrolateral preoptic nucleus) is only poorly

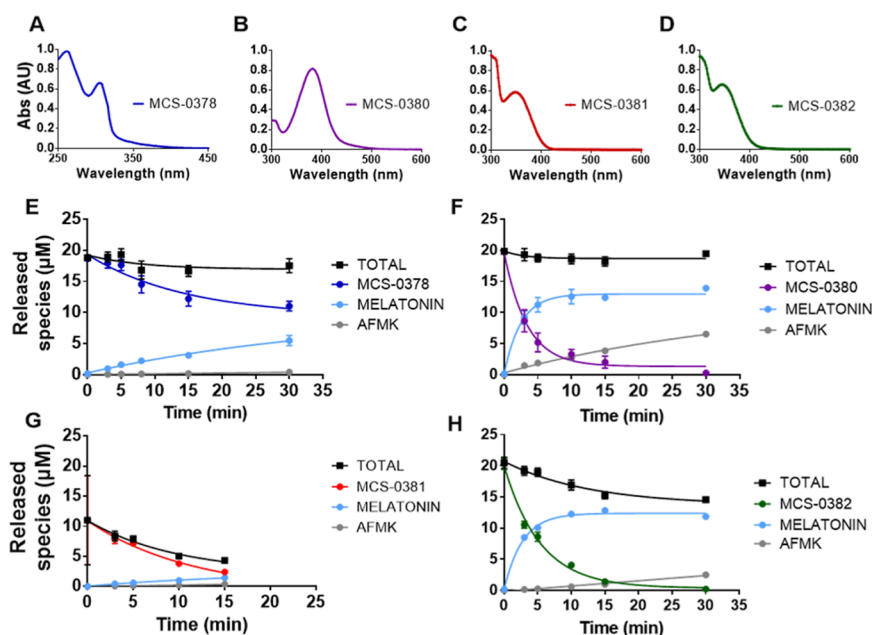


Figure 2. Photochemical characterization of compounds MCS-0378, MCS-0380, MCS-0381, and MCS-0382. UV-vis absorption spectra of MCS-0378 (A), MCS-0380 (B), MCS-0378 (C), and MCS-0382 (D), recorded in a 50 μM solution in 100% DMSO. Photolysis of compounds MCS-0378 (E), MCS-0380 (F), MCS-0381 (G), and MCS-0382 (H) performed at $\lambda = 405$ nm in a 20 μM solution in PBS/DMSO (98:2). AFMK: *N*¹-acetyl-*N*²-formyl-5-methoxykynuramine. Data are expressed as mean \pm SEM of three independent experiments.

defined.¹² Light activation in specific brain regions followed by electroencephalogram/electromyogram (EEG/EMG) recordings is likely to provide new insights in this respect. A similar approach can be envisioned to better define the brain regions involved in the regulation of pain by melatonin.¹³ Melatonin has been also shown to regulate glucose homeostasis, but whether this occurs through peripheral or central effects remains poorly known.¹⁴ Indeed, melatonin is known to regulate the circadian rhythm of the biological master clock located in the hypothalamic suprachiasmatic nucleus and to affect glucose homeostasis by directly acting on glucose sensitive peripheral organs such as the liver or the pancreas. Local activation of melatonin receptors is likely to detangle the respective contributions of these organs.

Using the well-known *o*-nitrobenzyl (*o*-NB) and coumarin photocleavable groups, we have developed here the first family of caged melatonin ligands, with the objective to modulate the activation of melatonin receptors in a light-controlled manner *in vitro* and *in vivo*.

RESULTS AND DISCUSSION

Design and Chemical Synthesis of Caged Melatonin Compounds. A successful design of a caged compound is based on the attachment of a light-sensitive moiety or photocleavable-protecting group (PPG) in a region of the active molecule that is relevant for ligand recognition and activation of the target receptor.^{7,15} Our initial objective was to design a caged derivative of melatonin suitable to release this biomolecule upon illumination in biological environments. Structure-activity relationship (SAR) studies on melatonin receptors revealed the importance of the methoxy substituent at the C5 position of melatonin and the alkylamide side chain on the intrinsic activity and high binding affinity to its receptors.^{1,16-19} However, selective attachment of the PPG to the acetamide side chain was not considered initially a good approach due to the recognized difficulties in amide photo-

release.²⁰ In spite of the fact that some solutions have been found for caging primary amides,²¹⁻²⁴ no reports support its use in the release of secondary amides such as melatonin. Moreover, attachment of the PPG at the C5 methoxy was also discarded due to the inexistence of chemical modifications of this group amenable to its photorelease. Therefore, we considered alternatives at other positions of melatonin that could present higher reactivity, as in the case of *N*1. On one hand, the presence of relatively bulky groups at the *N*1-position decreases the affinity of a ligand for both melatonin receptors, without displaying selectivity toward *MT*₁ or *MT*₂.²⁵⁻²⁷ On the other hand, indolic nitrogen can be chemically modified with different groups. Therefore, *N*1 was the selected position for the introduction of the caging groups in the structure of these caged melatonin derivatives (Figure 1).

We aimed to design three compounds (MCS-0378, MCS-0380, and MCS-0381) containing a carbamate linker between melatonin and the caging group and one compound (MCS-0382) presenting a 4,5-dimethoxy-2-nitrobenzyl (DMNB) group directly attached to melatonin by *N*1-benylation. Although the literature on *N*1-*o*-nitrobenzyl-protected indole derivatives is scarce, the contradictory reports on the efficiency of indole photorelease from these precursors^{28,29} prompted us to consider direct alkylation of melatonin indolic nitrogen as a possible alternative to carbamates. The benzylated melatonin analogue MCS-0382 was obtained in low to moderate yields after deprotonation of melatonin with sodium hydride, followed by the rapid addition of DMNB-bromide in DMF at low temperature (Scheme 1A). The competitive *N*-benzylation of melatonin acetamide and double alkylation were side reactions. Two different synthetic pathways were used to obtain the carbamate derivatives, as shown in Scheme 1B,C. In the first reaction, a two-step, one-pot *N*-acylation of indole was performed, following the methodology described by Macor et al. in 1999.³⁰ Accordingly, carbonyldiimidazole

(CDI) was used as an activating agent in the presence of a catalytic amount of 4-dimethylaminopyridine (DMAP). However, this procedure was only valid for the synthesis of MCS-0378, which was obtained in 15% overall yield. Poor yields were explained by the main formation of the dimer of melatonin, linked at the N1-position by a carbonyl group. In order to improve reaction efficiency, a second synthetic methodology was proposed (Scheme 1C). In this reaction, CDI was substituted with 4-nitrophenyl chloroformate in the first step of the synthesis, avoiding the side reaction of melatonin dimerization. The obtained intermediate then reacted with the benzyl alcohol derivative of DMNB or diethylaminocoumarin (DEAC) in ACN, in the presence of catalytic DMAP. These conditions improved slightly the overall yield of the synthesis, and compounds MCS-0380 and MCS-0381 were finally obtained in 26 and 53% yields, respectively. Optimization of the synthetic procedures for these compounds was not performed due to the lower photochemical performances of the carbamate-linked melatonin derivatives. The subnanomolar activity of melatonin at MT₁ and MT₂ receptors requires efficient exhaustive purification of the caged derivatives to secure the absence of this bioactive compound in the samples used for biological testing.

Another important aspect to consider is the release of side products upon uncaging.¹⁵ For instance, photolytic cleavage of the *o*-NB-based PPGs yields multiple nitrosobenzene derivatives,³¹ whose possible interference with the biological system must be determined. Similarly, the coumarin-containing PPGs generate the corresponding benzyl alcohol.³² In order to test the eventual effect of the cage photolytic products on melatonin receptors in cells, three light-sensitive phosphate derivatives were synthesized, one for each caging group described herein (*o*-NB, DMNB, and DEAC) that release phosphate upon illumination. Details on the synthesis of these molecules are provided on the Supporting Information (scheme S2).

Photochemical Characterization of Caged Melatonin Compounds. UV–Vis absorption spectra was recorded for each compound, in order to determine the interval of wavelengths that promote the uncaging process. Compound MCS-0378 showed two absorption peaks at $\lambda = 260$ nm and $\lambda = 306$ nm (Figure 2A), which are concordant with the presence of an *o*-NB moiety. Compound MCS-0380 displayed an absorption maximum of $\lambda = 380$ nm (Figure 2B), consistent with the higher absorption wavelengths of coumarin-based PPGs. DMNB-type compounds MCS-0381 and MCS-0382 are based on a *o*-NB derivative, but they present two additional methoxy groups in their structure, which are electron-donating groups (EDGs) that induce a slight bathochromic shift. Therefore, the absorption maxima of these compounds are displaced to longer wavelengths in comparison to MCS-0378, with two clear absorption maxima at $\lambda = 306$ nm and $\lambda = 350$ nm for both cases (Figure 2C,D).

Considering the information extracted from the UV–vis spectra of different compounds, the photolytic process should be triggered with light of wavelengths ranging from 320 to 400 nm. To avoid the toxicity and cell damage effects associated with UV light, we used a laser with a wavelength in the visible spectrum range ($\lambda = 405$ nm and 2.37 mW/mm²).

We then monitored photolysis and light stability under conditions similar to those used in biological assays. Aqueous solutions of the caged compounds were illuminated for different periods of time and subsequently analyzed by

HPLC-MS. For each time point, we quantified the amount of released melatonin and verified the formation of side products (Figure 2E–H). Interestingly, apart from the expected release of melatonin, we detected the formation of a unique photolysis product, which was identified as *N*¹-acetyl-*N*²-formyl-5-methoxykynuramine (AFMK). AFMK is the main product of the oxidative metabolism of melatonin, and it presents well-established antioxidant properties.³⁴ Its formation involves a pyrrole ring oxidative cleavage of melatonin,³⁵ a process that is favored by the action of light.³⁶ Therefore, the AFMK concentration was systematically monitored, revealing a minor formation of this photo-oxidation product under our assay conditions (Figure 2E–H, gray lines; Figure S1). Concentrations of the different species in the sample were calculated with the equation extracted from the calibration curve for each analyte (Figure S2).

Compound MCS-0378 did not present a complete uncaging (Figure 2E) as it mainly remained in its caged form even after long light exposures, consistent with its absorption maxima at lower wavelengths. Consequently, the amount of released melatonin at 405 nm was not prominent, reaching concentrations below 5 μ M after applying light for 15 min to a 20 μ M solution. Interestingly, no photolytic degradation was detected under these conditions.

Compounds MCS-0380 and MCS-0382 presented similar uncaging rates and photostability (Figure 2F,H), with a photolytic reaction that was completed after 15 min. In both cases, melatonin was released with relatively high uncaging efficiencies after 5 min of irradiation, detecting concentrations between 10 and 13 μ M (corresponding to 50 and 65% of the theoretical conversion, respectively). However, melatonin does not entirely account for the phototransformed compound MCS-0382 (Figure 2H). This can be due to the formation of undefined intermediates upon photolysis of *o*-NB-derivatives³³ or due to the partial reaction of melatonin with the nitrosoaldehyde intermediate, as reported in the N1-nitrobenzyl photolytic deprotection of indoles.²⁸ Nevertheless, properties of compound MCS-0382 are remarkable, not only for the high uncaging yields upon light exposure but also for its chemical stability and improved solubility in aqueous media.

In contrast, the amount of released melatonin from the compound MCS-0381 was lower than expected (Figure 2F), with concentrations that oscillated between 1 and 2 μ M after 15 min of light exposure. In addition to unfavorable photochemical properties, this compound was poorly water-soluble, requiring high percentages of organic solvent (higher than 20%) to avoid precipitation. Overall, these properties hindered the study of the uncaging process and seriously limited the applicability of MCS-0381 to further in vitro studies in cells.

Affinity of Caged Melatonin Compounds for MT₁ and MT₂ Receptors. The affinity of the caged compounds for human melatonin MT₁ and MT₂ receptors stably expressed in HEK293 cells was determined in competition binding assays with 2-[¹²⁵I]iodomelatonin (2-[¹²⁵I]-MLT), under dark conditions and after the pre-illumination of the caged compounds for 15 min at 405 nm. The reference compound melatonin showed the expected sub-nanomolar affinity for MT₁ and MT₂ (pK_i = 9.56 ± 0.29 and 9.76 ± 0.45, respectively). All caged compounds presented the expected reduction (>100-fold) in binding affinity, with the exception of compound MCS-0380, which maintained an intermediate affinity for MT₂ with a pK_i of 8.34 ± 0.50 (Table 1). The

Table 1. Affinity and Agonist Potency of MCS-0378, MCS-0380, MCS-0381, and MCS-0382 in HEK293 Cells Stably Expressing MT₁ and MT₂

ligand	pK _i ± S.E.M.		pEC ₅₀ ± S.E.M. (E _{max})	
	MT ₁	MT ₂	MT ₁	MT ₂
melatonin	9.56 ± 0.29	9.76 ± 0.45	10.16 ± 0.15	9.76 ± 0.45
MCS-0378	6.83 ± 0.17	7.86 ± 0.33	8.90 ± 0.36 (42 ± 6)	6.72 ± 0.42
MCS-0378 + light	8.63 ± 0.34	8.70 ± 0.34	9.21 ± 0.16	8.89 ± 0.22
MCS-0380	7.46 ± 0.55	8.34 ± 0.50	9.23 ± 0.32 (46 ± 6)	7.47 ± 0.33
MCS-0380 + light	8.74 ± 0.14	8.66 ± 0.05	9.35 ± 0.16	9.19 ± 0.17
MCS-0381	7.29 ± 0.06	7.40 ± 0.11	n.d.	n.d.
MCS-0381 + light	8.11 ± 0.01	8.16 ± 0.07	n.d.	n.d.
MCS-0382	6.32 ± 0.23	6.56 ± 0.19	6.83 ± 0.23	8.03 ± 0.30 (39 ± 5)
MCS-0382 + light	8.90 ± 0.22	9.16 ± 0.23	9.59 ± 0.13	9.38 ± 0.25

highest shift in affinity (1000-fold) was observed for **MCS-0382** with pK_i values in the micromolar range (pK_i = 6.32 ± 0.23 and 6.56 ± 0.19 for MT₁ and MT₂, respectively).

The affinity was measured in 2-[¹²⁵I]-MLT competition experiments and is expressed as mean pK_i ± S.E.M. Agonist potency was measured as inhibition of forskolin-stimulated cAMP production and is expressed as pEC₅₀ ± S.E.M. Values obtained with light-activated compounds correspond to apparent pK_i and pEC₅₀. Maximal efficacy of the ligands, E_{max} is expressed as a percentage of the maximal effect observed with melatonin (=100%). Data correspond to the mean of at least three independent experiments, each of them performed using at least eight different ligand concentrations. n.d., not determined.

Upon illumination of the caged compounds for 10 min, an increase in apparent affinity was observed on both receptors, confirming the light-mediated generation of biologically active melatonin. Remarkably, in the formation of AFMK upon light exposure, melatonin activity was not affected as pK_i values remained unchanged (Table S1). The increase in the apparent affinity correlates with the uncaging efficiency of each compound and the amount of melatonin generated. Accordingly, compound **MCS-0382** presented the most promising properties, with the highest apparent affinity shift from the micromolar range under dark conditions to the low nanomolar range upon uncaging (Figure 3G,H, Table 1). In contrast, compounds with inferior uncaging efficiencies, like compound **MCS-0381**, did not show an important increase in apparent affinity after uncaging, consistent with the lower amount of released melatonin observed for this compound (Figure 3E,F, Table 1). Compounds **MCS-0378** and **MCS-0380** displayed a moderate increase in apparent affinity after light application (Figure 3A–D). The narrow window in affinity difference between dark and light conditions of **MCS-0378** and **MCS-0380** is most likely due to the modest loss of affinity by the introduction of the caging groups.

To exclude any impact of other photolytic products generated during the course of the uncaging reaction, we determined the affinity of AFMK and the caging groups for melatonin receptors, before and after light application. Neither the phosphate derivatives of the caging groups (Figure S4) nor AFMK (Figure S5) showed any significant interference at concentrations up to 1 μM. These results exclude any significant impact of these photolytic products on the pharmacological properties of uncaged melatonin on MT₁ and MT₂ receptors.

In conclusion, we generated several caged melatonin compounds with variable uncaging efficiencies upon light

illumination. The apparent affinity of uncaged melatonin for MT₁ and MT₂ receptors is governed by the uncaging efficiency of each compound, and no significant interferences of the released cage moiety or photolytic side products could be detected. The dimethoxynitrobenzyl compound **MCS-0382** shows the most interesting properties with an affinity shift of almost 3 logs upon light illumination on MT₁ and MT₂ receptors, useful for biological applications. Its apparent affinity close to pure melatonin is in good accordance to its high uncaging efficiency (65%, 10 min, 405 nm, and 2.37 mW/mm²) and was selected for cell assays due to the optimal photochemical and receptor affinity properties.

Functional Activity of Caged Melatonin Compounds on MT₁ and MT₂ Receptors. The well-documented property of melatonin receptor agonists to inhibit intracellular cAMP production was used as a functional readout for our compounds. All caged melatonin compounds presented agonistic properties, that is, inhibited forskolin-stimulated cAMP production for MT₁ and MT₂ receptors prior to light activation (Table 1), whereas pure melatonin showed expected EC₅₀ values in the sub-nanomolar range; EC₅₀ values for caged compounds were 1–3 logs higher (Table 1). **MCS-0378** and **MCS-0380** were partial agonists for MT₁, and full agonists for MT₂ (Figure 4A–D). In contrast, **MCS-0382** behaved as full agonists for MT₁ and as partial agonists for MT₂ (Figure 4E,F). Upon light activation at 405 nm, all compounds became full agonists for both receptors in accordance with the generation of melatonin through uncaging. Apparent EC₅₀ values correlated with the uncaging efficiency of each compound (Table 1). For **MCS-0382**, apparent EC₅₀ values were close to those of pure melatonin, in agreement with its excellent uncaging efficiency of 65%.

Electrophysiological Analysis of in Situ Uncaging of MCS-0382 in SCN Neurons. We then evaluated the biological activity of the melatonin generated from **MCS-0382** upon light illumination in rat SCN brain slices by monitoring its effect on neuronal excitability in whole-cell recordings. Similar to the reported effect of melatonin in this system at ZT6-11,^{37–39} most SCN neurons (*n* = 14/21) responded to the application of light-activated **MCS-0382** (Figure 5). Six of 21 neurons showed a hyperpolarization response (Figure 5A) and 8/21 showed a depolarization response (Figure 5B), while 7/21 remained unresponsive (Figure 5C). This heterogeneity resembles that known for pure melatonin and reflects the proportion of melatonin receptor-expressing neurons and the direct and indirect effect of melatonin on neuronal polarization through the modulation of inhibitory GABAergic transmission.³⁹

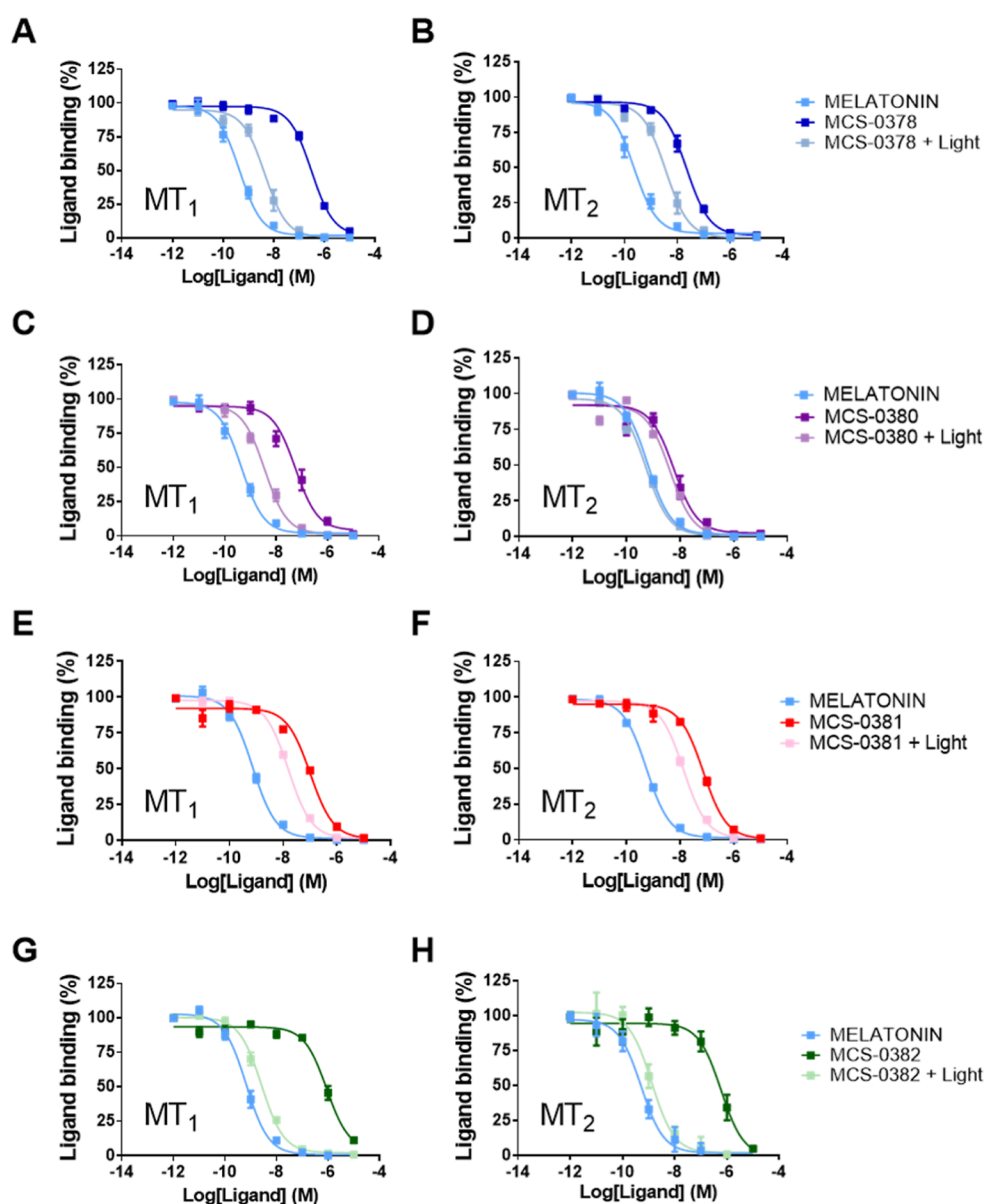


Figure 3. Competition of 2-[¹²⁵I]-MLT binding with melatonin, MCS-0378, MCS-0380, MCS-0381, and MCS-0382 before and after light exposure, in crude membranes from HEK293 cells expressing MT₁ or MT₂ receptors. Light is applied to the ligands for 10 min prior to incubation with the membranes, using a laser as a light source (405 nm, 2.37 mW/mm²). Data are expressed as mean ± SEM from three to five independent experiments [(A) melatonin *n* = 4, MCS-0378 (dark) *n* = 3, MCS-0378 (light) *n* = 3; (B) melatonin *n* = 5, MCS-0378 (dark) *n* = 3, MCS-0378 (light) *n* = 3; (C) melatonin *n* = 4, MCS-0378 (dark) *n* = 3, MCS-0378 (light) *n* = 3; (D) melatonin *n* = 4, MCS-0380 (dark) *n* = 4, MCS-0380 (light) *n* = 3; (E) melatonin *n* = 4, MCS-0380 (dark) *n* = 3, MCS-0380 (light) *n* = 3; (F) melatonin, MCS-0380 (dark), MCS-0380 (light), MCS-0381 (dark), MCS-0381 (light) *n* = 3; (G) melatonin *n* = 5, MCS-0382 (dark) *n* = 5, MCS-0382 (light) *n* = 4; (H) melatonin *n* = 5, MCS-0382 (dark) *n* = 5, MCS-0382 (light) *n* = 3]. Data are represented as percentage of maximal binding in the absence of compounds and normalized to the melatonin maximum effect.

Our caged melatonin compounds present not only a proof-of-concept for the feasibility of melatonin as a photopharmacological tool but also for the development of other photo-activatable molecules and sub-type selective melatonin receptor ligands. For instance, melatonin derivatives containing caging groups that undergo photolysis at longer and even less invasive wavelengths can be envisioned,⁵⁰ such as BODIPY⁵¹ or the melatonin moiety replaced with an antagonistic or receptor type-selective molecule.¹⁰ Caged MT₁- and MT₂-selective molecules would be of particular interest to further decipher the specific and opposing effects of the two melatonin receptors on sleep.⁴⁰ A further development of our caged melatonin compounds could be the attachment of moieties

that target specific subcellular compartments. The latter provides a higher degree of optical control, and it has been previously applied to release caged lipids from organelles such as mitochondria, lysosomes, or endoplasmic reticulum.^{41,42} Subcellular compartment-targeted molecules might be of particular interest to study the role of the previously described mitochondrial MT₁ receptors.^{43,44}

CONCLUSIONS

In this work, we describe the synthesis and functional characterization of the first family of photo-activatable melatonin receptor ligands. Following the caging strategy, three different PPGs have been selected to generate

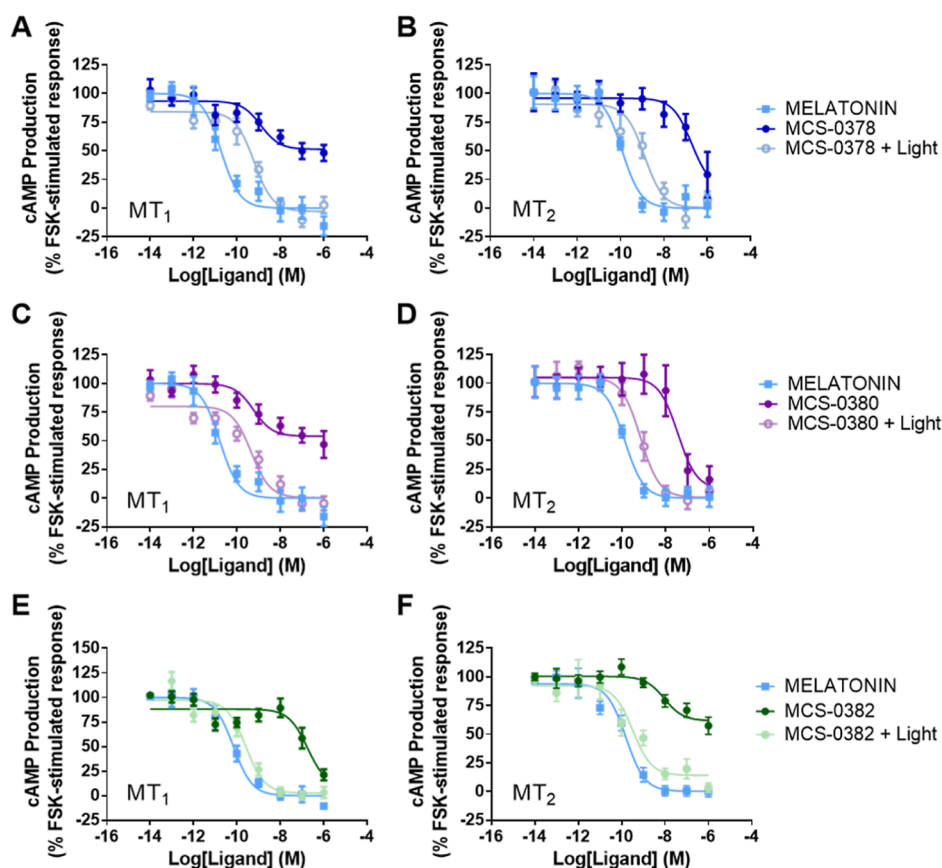


Figure 4. Inhibition of cAMP production by melatonin and compounds MCS-0378, MCS-0380, and MCS-0382 before and after light exposure in cells stably expressing MT₁ (A,C,E) and MT₂ (B,D,F). Light is applied to the ligands for 10 min prior to incubation with the cells, using a laser as a light source (405 nm, 2.37 mW/mm²). Data are expressed as mean \pm SEM from four to eight independent experiments [(A) melatonin $n = 7$, MCS-0378 (dark) $n = 7$, MCS-0378 (light) $n = 7$; (B) melatonin $n = 5$, MCS-0378 (dark) $n = 5$, MCS-0378 (light) $n = 5$; (C) melatonin $n = 7$, MCS-0380 (dark) $n = 7$, MCS-0380 (light) $n = 7$; (D) melatonin $n = 5$, MCS-0380 (dark) $n = 5$, MCS-0380 (light) $n = 5$; (E) melatonin $n = 8$, MCS-0382 (dark) $n = 8$, MCS-0382 (light) $n = 4$; (F) melatonin $n = 4$, MCS-0382 (dark) $n = 4$, and MCS-0382 (light) $n = 3$]. Data are presented as percentage of forskolin-stimulated response and normalized to the maximal and minimal melatonin effect. The amplitude of cAMP inhibition before normalization varied between 50 and 75%.

compounds MCS-0378, MCS-0380, MCS-0381, and MCS-0382 by attachment of the caging group at the N1 position of melatonin. With the exception of MCS-0381, all compounds release active melatonin with relatively high yields, which is reflected by the excellent apparent EC₅₀ values for the inhibition of cAMP production of the compounds upon 405 nm illumination. The presence of the caging groups induced an important decrease in binding affinity of caged melatonin compounds for both receptors, giving 2–3 log concentration windows that are useful for light experiments in cells and tissues. These results reveal the importance of N1 substitution for the development of non-selective low-affinity ligands for melatonin receptors. MCS-0382 showed the most interesting properties as it is chemically stable, highly soluble in aqueous media, and displays an excellent uncaging efficiency and a more than 100-fold difference in affinity before and after photolysis. The biological activity of melatonin generated through light-induced uncaging was demonstrated in two cellular assays (ligand binding and signaling assays) and in rat SCN brain slices. Collectively, these results validate the caged melatonin derivative MCS-0382 as a photopharmacological tool for cellular and physiological studies.

EXPERIMENTAL SECTION

Organic Synthesis. All chemicals and solvents were obtained from commercial sources and used without purification, except anhydrous solvents, which were previously treated with a system of solvent purification (*PureSolvEN*), degassed by purging with inert gases, and dried over molecular sieves. Reactions were monitored by thin-layer chromatography (TLC) on silica gel (60 F, 0.2 mm, ALUGRAM Sil G/UV₂₅₄ Macherey-Nagel) by visualization under a 254 and/or 365 nm lamp. Compounds without chromophores were visualized using an ethanolic solution of phosphomolybdic acid by heating. Alternatively, nuclear magnetic resonance (NMR) was also used as a technique for reaction monitoring. When purification was required, *flash* column chromatography was performed on silica gel 60 (Panreac, 40–63 μ m RE). Reverse-phase column *flash* chromatography was performed on silica-gel C18 (SNAP KP-C18-HS, 50 μ m, Biotage) and automated with *Isolera One* with UV–vis detection (*Biotage*).

Compound characterization by NMR spectroscopy was performed with a *Variat-Mercury* 400 MHz spectrometer. Chemical shifts δ are reported in parts per million (ppm) using tetramethylsilane as an internal standard and using the residual non-deuterated solvent signal as reference [chloroform-*d* δ 7.26 ppm (¹H), δ 77.16 ppm (¹³C); methanol-*d*₄ δ 4.87 ppm, δ 3.31 ppm (¹H), δ 49.3 ppm (¹³C)]. The following abbreviations were used to designate multiplicities: s = singlet, d = doublet, t = triplet, q = quartet, m = multiplet, q = quintuplet, br = broad, dd = double-doublet, ddd = double-double-doublet, dt = double-triplet, td = triple-doublet. Coupling constants

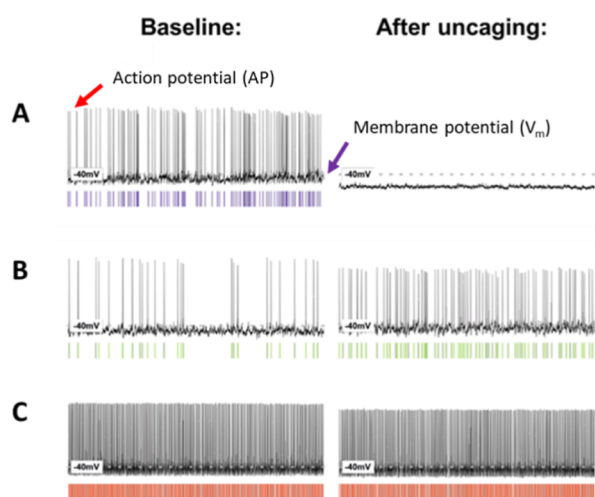


Figure 5. Effects of the application of light on the compound **MCS-0382** on the membrane properties of rat suprachiasmatic nuclei (SCN) neurons. (A) Some neurons responded to the light-mediated generation of melatonin with hyperpolarization ($n = 6/21$), accompanied by a decrease or elimination of the spontaneous firing rate. (B) Other neurons responded to the light-mediated generation of melatonin with a depolarization ($n = 8/21$), accompanied by an increase in the spontaneous firing rate. (C) Remaining neurons did not respond to the light-mediated release of melatonin ($n = 7/21$). Using the laser (405 nm, 2.37 mW/mm²), 1 μ M **MCS-0382** was pre-illuminated for 10 min prior to application.

(J) were expressed in Hz. Signals were assigned as far as possible by means of two-dimensional NMR spectroscopy: 1H–1H–COSY, HSQC, and HMBC.

Purity of compounds was >95%, and it was determined by HPLC using two different methods (method A and method B). In both cases, purity is given as % absorbance at 254 nm.

Method A was performed using a *Dionex Ultimate 3000SD* HPLC system (*Thermo Fischer Scientific*), which was coupled to a PDA detector and to a mass spectrometer *LTQ XL ESI-ion trap* (*Thermo Fischer Scientific*). For this method, the column used was *ZORBAX Extend C18* (2.1 \times 50 mm, 3.5 μ m; P.N. 735700–902). The flow rate was 0.9 mL/min, column temperature was fixed to 30 $^{\circ}$ C, and total runtime was 10 min. The mobile phase used was a mixture of A = formic acid 0.05% in water and B = formic acid 0.05% in acetonitrile (ACN), with the method described as follows: from 5% B to 90% B in 5 min, 90% B for 2 min, from 90% B to 100% B in 1 min, and 100% B for 2 min. UV–vis spectra were collected every 0.2 s between 190 and 800 nm, and bands show % maximal absorbance. Data from mass spectra were analyzed by electrospray ionization in positive and negative modes between 50 and 2000 Da, using *Xcalibur* software version 2.2 (*Thermo Fischer Scientific*). Method B was performed using a *Waters2795 Alliance* HPLC system, coupled to a DAD detector (*Agilent 1100*) and to an *ESI Quattro micro MS* detector (*Waters*). For this method, the column used was *ZORBAX Eclipse Plus C18* (4.6 \times 150 mm, 3.5 μ m). The flow rate was 0.5 mL/min, column temperature was fixed to 35 $^{\circ}$ C, and total runtime was 10 min. The mobile phase used was a mixture of A = formic acid 0.05% in water and B = formic acid 0.05% in ACN, with the method described as follows: 5% B for 0.5 min, from 5% B to 100% B in 5 min, 100% B for 1.5 min, from 100% B to 5% B in 1 min, and 5% B for 2 min. UV–vis spectra were collected every 0.2 s between 210 and 600 nm and bands show % maximal absorbance. Data from mass spectra were analyzed by electrospray ionization in positive and negative modes every 0.3 s between 150 and 1500 Da, using *MassLynx* software version 4.1 (*Waters*).

High-resolution mass spectra and elemental composition were analyzed by FIA (flux injected analysis) using ultrahigh-performance liquid chromatography (UPLC) *Aquity* (*Waters*) coupled to a LCT

premier orthogonal accelerated time-of-flight mass spectrometer (TOF) (*Waters*). Data from mass spectra were analyzed by electrospray ionization in positive and negative modes using *MassLynx* software version 4.1 (*Waters*). Spectra were scanned between 50 and 1500 Da with values every 0.2 s and peak values are given in m/z . Melting points were taken using open capillary tubes and measured with a melting point B-545 (*Büchi*) system, ramp 0.5 $^{\circ}$ C/min with a digital temperature measurement. IR spectra were registered in chloroform solution and recorded using a *Thermo Nicolet Avatar 360 FT-IR* spectrometer.

2-Nitrobenzyl 3-(2-acetamidoethyl)-5-methoxy-1H-indole-1-carboxylate (MCS-0378). To a solution of commercially available melatonin (90 mg, 0.38 mmol, 1 equiv) in dry ACN (0.2 M) under an inert atmosphere, a solution of di(1H-imidazol-1-yl)methanone (70.4 mg, 0.42 mmol, 1.1 equiv) and *N,N*-dimethylpyridin-4-amine (11.6 mg, 0.09 mmol, 0.25 equiv) in dry ACN (4.4 mL) was added dropwise at room temperature. The mixture was stirred for 30 min at 40 $^{\circ}$ C, and a solution of 2-nitrobenzyl alcohol (83 mg, 0.53 mmol, 1.4 equiv) in dry ACN (0.5 mL, 1 M) was then added. The resulting solution was heated under reflux with magnetic stirring for 2 days. The reaction was then completed and quenched with HCl 1 M (30 mL), and the aqueous layer was extracted with EtOAc (4 \times 25 mL). Combined organic layers were washed with brine (2 \times 40 mL), dried over anhydrous Na₂SO₄, filtered, and evaporated under reduced pressure. The crude product was first purified by column chromatography through silica gel using DCM/MeOH (98:2), in order to discard the benzyl bromide derivatives and melatonin. The product-containing fractions were re-purified by column chromatography through silica gel using DCM/MeOH (97:3), giving the expected product as a white solid (22.3 mg, 15%).

¹H NMR (400 MHz, chloroform-*d*): δ 8.15 (d, $J = 8.2$ Hz, 1H), 8.04 (s, 1H), 7.71–7.67 (m, 2H), 7.55 (ddd, $J = 8.6, 5.5, 3.3$ Hz, 1H), 7.42 (s, 1H), 7.01 (d, $J = 2.5$ Hz, 1H), 6.96 (dd, $J = 8.9, 2.5$ Hz, 1H), 5.83 (s, 2H), 5.64 (s, 1H), 3.87 (s, 3H), 3.59 (q, $J = 6.5$ Hz, 2H), 2.89 (t, $J = 6.8$ Hz, 2H), 1.97 (s, 3H). ¹³C NMR (101 MHz, chloroform-*d*): δ 170.38 (2C), 156.53 (2C), 134.09, 131.48 (2C), 129.57 (2C), 125.41, 119.26 (2C), 116.23, 113.71, 102.14, 65.24, 55.93, 39.08, 25.31, 23.52. HPLC-PDA-MS (using method A): RT = 2.66 min, $\lambda_{\max} = 209, 243, 299$ nm; purity 98% (254 nm). HRMS calculated for C₂₁H₂₂N₃O₆: 412.1509 [M + 1]⁺; found, 412.1489; mp 133.2–133.8 $^{\circ}$ C.

4-Nitrophenyl 3-(2-Acetamidoethyl)-5-methoxy-1H-indole-1-carboxylate (1). To a solution of commercially available melatonin (96 mg, 0.40 mmol) in dry ACN (1.5 mL, 0.3 M) under an inert atmosphere, a solution of 4-nitrophenyl chloroformate (105 mg, 0.50 mmol) in dry ACN (0.5 mL, 1 M), a solution of DMAP (12.34 mg, 0.10 mmol) in dry ACN (0.2 mL, 0.5 M), and triethylamine (70 μ L, 0.50 mmol) were added dropwise. The resulting mixture was heated under reflux overnight with magnetic stirring. The reaction was then quenched with HCl 1 M (50 mL), and the aqueous layer was extracted with EtOAc (4 \times 25 mL). Combined organic layers were washed with brine (2 \times 40 mL), dried over anhydrous Na₂SO₄, filtered, and evaporated under reduced pressure. The crude product was purified by column chromatography through silica gel using DCM/MeOH (98:2), giving the expected product as beige crystals (78 mg, 49%).

¹H NMR (400 MHz, chloroform-*d*): δ 8.39–8.30 (m, 2H), 8.08 (s, 1H), 7.53 (s, 1H), 7.52–7.46 (m, 2H), 7.07 (d, $J = 2.4$ Hz, 1H), 6.99 (dd, $J = 9.0, 2.5$ Hz, 1H), 5.70 (s, 1H), 3.89 (s, 3H), 3.62 (q, $J = 6.7$ Hz, 2H), 2.93 (t, $J = 7.0$ Hz, 2H), 1.98 (s, 3H). ¹³C NMR (101 MHz, chloroform-*d*): δ 170.37, 156.94, 154.94, 145.80, 131.73, 130.13, 125.55 (2C), 122.81, 122.50 (3C), 120.43, 116.33, 113.92, 102.50, 55.92, 39.12, 25.41, 23.51. HPLC-PDA-MS (using method B): RT = 3.55 min, $\lambda_{\max} = 210, 244, 263, 300$ nm; purity 95% (254 nm). HRMS calculated for C₂₀H₂₀N₃O₆: 398.1352 [M + 1]⁺; found, 398.1356; mp 182.1–182.2 $^{\circ}$ C.

(7-(Siethylamino)-2-oxo-2H-chromen-4-yl)methyl-3-(2-acetamidoethyl)-5-methoxy-1H-indole-1-carboxylate (MCS-0380). To a stirred solution of 4-nitrophenyl 3-(2-acetamidoethyl)-5-methoxy-1H-indole-1-carboxylate **1** (52 mg, 0.13 mmol, 1 equiv) in dry ACN

(1 mL) under an argon atmosphere, a solution of DEAC-OH (38 mg, 0.14 mmol, 1.3 equiv) and *N,N*-BrB was added. The mixture was immediately protected from light and heated under reflux under magnetic stirring for 3 days. Then, the reaction was quenched with a HCl 1 M solution (50 mL), and the aqueous layer was extracted with EtOAc (4 × 25 mL). Combined organic layers were dried over anhydrous Na₂SO₄, filtered, and evaporated under reduced pressure. The crude product was first purified by column chromatography through silica gel using DCM/MeOH (97:3), in order to discard the benzyl derivatives and melatonin. The product-containing fractions were re-purified using the same conditions as before, DCM/MeOH (98:2), giving the expected product as a yellow solid (35 mg, 53%).

¹H NMR (400 MHz, chloroform-*d*): δ 8.06 (s, 1H), 7.44 (s, 1H), 7.37 (d, *J* = 8.9 Hz, 1H), 7.04 (d, *J* = 2.5 Hz, 1H), 6.96 (dd, *J* = 9.0, 2.5 Hz, 1H), 6.62 (dd, *J* = 9.0, 2.6 Hz, 1H), 6.54 (d, *J* = 2.6 Hz, 1H), 6.20 (s, 1H), 5.62 (s, 1H), 5.53 (s, 2H), 3.87 (s, 3H), 3.59 (q, *J* = 6.6 Hz, 2H), 3.43 (q, *J* = 7.1 Hz, 4H), 2.90 (t, *J* = 6.9 Hz, 2H), 1.97 (s, 3H), 1.21 (d, *J* = 7.0 Hz, 6H). ¹³C NMR (101 MHz, chloroform-*d*): δ 170.34, 161.82, 156.61, 156.48, 150.71, 148.92, 131.47, 124.55, 122.88, 119.65 (2C), 116.19 (2C), 113.83, 109.18, 107.00, 105.95, 102.22, 98.27, 63.67, 55.92, 45.09 (2C), 39.23, 25.34, 23.54, 12.54 (2C). HPLC-PDA-MS (using method B): RT = 3.83 min, λ_{max} = 210, 244, 386 nm; purity >98% (254 nm). HRMS calculated for C₂₈H₃₂N₃O₆: 506.2291 [M + 1]⁺; found, 506.2291; mp 173.1–173.6 °C.

4,5-Dimethoxy-2-nitrobenzyl 3-(2-acetamidoethyl)-5-methoxy-1H-indole-1-carboxylate (MCS-0381). To a stirred solution of 4-nitrophenyl 3-(2-acetamidoethyl)-5-methoxy-1H-indole-1-carboxylate **1** obtained in the first step (132 mg, 0.30 mmol, 1 equiv) in dry ACN (3 mL) under an argon atmosphere, a solution of 4,5-dimethoxy-2-nitrobenzyl alcohol (99 mg, 0.45 mmol, 1.3 equiv) and *N,N*-dimethylpyridin-4-amine (9.26 mg, 0.08 mmol, 0.25 equiv) in dry ACN (1 mL) was added. The mixture was immediately protected from light and heated under reflux under magnetic stirring for six days. Then, the reaction was quenched with a HCl 1 M solution (50 mL), and the aqueous layer was extracted with EtOAc (4 × 25 mL). Combined organic layers were dried over anhydrous Na₂SO₄, filtered, and evaporated under reduced pressure. The crude product was first purified by column chromatography through silica gel using DCM/EtOAc (95:5), in order to discard the benzyl derivatives and melatonin. The product-containing fractions were re-purified using the same conditions as before: DCM/MeOH (98:2), giving the expected product as a pale-brown solid (37.5 mg, 26%).

¹H NMR (400 MHz, chloroform-*d*): δ 8.04 (s, 1H), 7.75 (s, 1H), 7.42 (s, 1H), 7.10 (s, 1H), 7.01 (d, *J* = 2.0 Hz, 1H), 6.95 (dd, *J* = 9.0, 2.5 Hz, 1H), 5.82 (s, 2H), 5.60 (s, 1H), 3.97 (s, 3H), 3.95 (s, 3H), 3.87 (s, 3H), 3.58 (q, *J* = 6.6 Hz, 2H), 2.88 (t, *J* = 6.9 Hz, 2H), 1.96 (s, 3H). ¹³C NMR (101 MHz, chloroform-*d*): δ 170.37, 156.50, 153.46, 148.93, 140.39, 131.36, 130.13, 125.93, 123.05, 122.85, 119.19, 116.19, 113.71, 111.59, 108.60, 102.12, 65.63, 56.70, 56.63, 55.92, 39.14, 25.32, 23.49. HPLC-PDA-MS (using method A): RT = 2.60 min, λ_{max} = 195, 244, 301, 344 nm; purity 97% (254 nm). HRMS calculated for C₂₃H₂₆N₃O₈: 472.1720 [M + 1]⁺; found, 472.1736; mp 205.7–206.3 °C.

***N*-(2-(1-(4,5-Dimethoxy-2-nitrobenzyl)-5-methoxy-1H-indol-3-yl)ethyl)acetamide (MCS-0382).** To a suspension of sodium hydride (17.82 mg, 0.45 mmol, 1.1 equiv) in dry DMF (1 mL, 0.45 M) under an argon atmosphere at 0 °C, a solution of commercially available melatonin (97 mg, 0.41 mmol, 1 equiv) in dry DMF (0.6 mL, 0.7 M) was added dropwise. The ice/water bath was removed, and the reaction was stirred for 2 h while the temperature increased to room temperature. Then, an excess of dry DMF (3.5 mL) was added, and the reaction was cooled to −40 °C with an acetone/dry ice bath. A solution of 1-(bromomethyl)-4,5-dimethoxy-2-nitrobenzene (150 mg, 0.53 mmol, 1.3 equiv) in dry DMF (0.9 mL, 0.6 M) was added dropwise into the brown mixture, and it was immediately protected from light. The reaction was stirred overnight without exceeding a temperature of 10 °C. The reaction was then quenched with water (25 mL), and the aqueous layer was extracted with EtOAc (3 × 25 mL). The organic layers were washed with brine (4 × 30 mL), dried

over anhydrous MgSO₄, filtered, and evaporated under reduced pressure. The crude product was first purified by column chromatography through silica gel using DCM/MeOH (95:5), in order to discard the benzyl derivatives and melatonin. The product-containing fractions were re-purified using DCM/EtOAc/MeOH (96:1:3) as eluents, giving the expected product as a pale-brown solid (61.3 mg, 35%).

¹H NMR (400 MHz, chloroform-*d*): δ 7.73 (s, 1H), 7.07 (d, *J* = 2.4 Hz, 1H), 7.03 (d, *J* = 8.9 Hz, 1H), 6.95 (s, 1H), 6.84 (dd, *J* = 8.9, 2.4 Hz, 1H), 5.80 (s, 1H), 5.70 (s, 1H), 5.67 (s, 2H), 3.93 (s, 3H), 3.86 (s, 3H), 3.58 (q, *J* = 6.6 Hz, 2H), 3.44 (s, 3H), 2.96 (t, *J* = 6.9 Hz, 2H), 1.96 (s, 3H). ¹³C NMR (101 MHz, chloroform-*d*): δ 170.26, 154.39, 154.06, 148.10, 139.51, 132.22, 129.57, 128.57, 127.05, 112.78, 112.75, 110.72, 109.70, 108.41, 101.04, 56.54, 56.19, 56.01, 48.20, 40.12, 25.49, 23.50. HPLC-PDA-MS (using method A): RT = 2.53 min, λ_{max} = 235, 282, 303, 344 nm; purity 98% (254 nm). HRMS calculated for C₂₂H₂₆N₃O₆: 428.1822 [M + 1]⁺; found, 428.1823; mp 131.3–131.4 °C.

Photochemistry. UV-vis absorption spectra of a 100 μM solution in DMSO of each compound were recorded using an Infinite M1000 Tecan microplate reader (λ = 250–800 nm). Irradiation experiments to trigger uncaging were performed in a 96-well white plate using a *BlueClassic* laser (TorLaser, Spain) to irradiate the samples from top (λ = 405 nm, 2.37 mW/mm²). All samples were prepared with a concentration of 20 μM in aqueous buffer, containing 2 to 10% DMSO depending on their solubility. 200 μL of these solutions were irradiated for different periods of time (t = 0, 3, 5, 8, 10, 15, and 30 min) and then analyzed by HPLC-MS to monitor photolysis. These analyses were performed on a *Dionex Ultimate 3000SD* HPLC system (*Thermo Fischer Scientific*), which was coupled to a PDA detector and to a mass spectrometer *LTQ XL ESI-ion trap* (*Thermo Fischer Scientific*). Conditions of the analysis were the same as those for method A (see the organic chemistry section). Calibration curves of all quantifiable species were determined in each experiment by analyzing a minimum of seven dilutions of each compound, prepared at different concentrations ranging from 0.2 to 50 μM. Curves were fit by plotting the peak area of the analyte versus the concentrations of the analyte with least-squares linear regression. All experiments were performed at least in triplicate.

Illumination Experiments. In order to study the binding affinity and functional properties under light conditions, solutions of the compounds were prepared in aqueous buffer, with concentrations ranging from 10 to 30 μM. 250 μL of solution was deposited in a 96-well white plate, and light was applied from top at each well individually, using the same laser source as for the uncaging experiments (see above). Immediately after illumination, the compound was added to the cell system. All the experiments were performed in the dark.

Cell Culture. HEK293 cells were grown in complete medium (Dulbecco's modified Eagle's medium supplemented with 10% (v/v) fetal bovine serum (FBS), 4.5 g/L glucose, 100 U/mL penicillin, 0.1 mg/mL streptomycin, and 1 mM glutamine) (Invitrogen, CA, USA). Cells were maintained at 37 °C (95% O₂ and 5% CO₂).

Crude Membrane Preparation. Crude membranes were prepared as previously described.^{45–47} The expression of MT₁ and MT₂ receptors in the crude membranes was quantified using BCA assay, using a Pierce BCA protein assay kit (*ThermoFischer Scientific*, Waltham, MA, USA) and following the manufacturer's instructions.

Radioligand Binding Experiments. Radioligand binding assays were performed in 75 mM Tris (pH 7.4), 12 mM MgCl₂, 5 mM EDTA, and 2-[¹²⁵I]-MLT as a radioligand (*PerkinElmer*, Waltham, MA, USA), using membranes extracted from HEK293 cells stably expressing human MT₁ or MT₂ receptors. Saturation binding experiments were performed in the range of 1–1000 pM, and specific binding was defined as binding displaced by 10 μM MLT. Competition curves were performed by simultaneous incubation of 200 pm 2-[¹²⁵I]-MLT and increasing concentrations of the respective ligands. Assays were carried out in duplicates for 120 at 37 °C, followed by a rapid filtration through glass fiber filters (*Whatman*, Clifton, NJ, USA). Filter-retained radioactivity was determined with a

γ -counter LB2111 system (Berthold Technologies, Bad Wildbad, Germany). Competition curves were fitted with a one-site non-linear regression to determine IC_{50} values, using GraphPad Prism software version 6.0 (San Diego, CA, USA). Data were represented as percentage of maximal binding in the absence of compounds and normalized to melatonin maximum effect. K_i values were calculated from IC_{50} values using the Cheng–Prusoff formula: $K_i = IC_{50}/[1 + (L/K_d)]$, where L represents the 2- $[^{125}I]$ -MLT concentration and K_d represents the dissociation constant obtained from the corresponding radioligand saturation assays. K_d values were 198 ± 30 and 211 ± 19 pM for MT_1 and MT_2 , respectively, obtained from three independent saturation binding experiments.

Accumulative cAMP Assay. The accumulative cAMP assay was performed as previously described,⁴⁸ using a CisBio cAMP- G_i kit (Cisbio Bioassays, Codolet, France). Briefly, HEK293 cells stably expressing MT_1 or MT_2 receptors were dispensed into a 384-well plate (5000 cells per well) and stimulated with 1 μ M forskolin in the presence of increasing concentrations of melatonin or the ligands of interest, in PBS buffer supplemented with 1 mM IBMX (Sigma-Aldrich, St Quentin, France) for 30 min at room temperature. Cells were then lysed for 1 h at room temperature, and cAMP levels were determined following the manufacturer's instructions. The plate was read using an Infinite F500 Tecan microplate reader. Data were fitted by non-linear regression to determine E_{max} and EC_{50} values and normalized to forskolin-induced response (100%) using GraphPad Prism software.

Animals. Male Sprague-Dawley rats (Charles River, UK), 28 to 35 days old, were housed with free access to standard chow and water in a temperature-controlled environment under 12/12 h light/dark conditions with lights on at 8 A.M. All procedures were performed in accordance with the U.K. Animals (Scientific Procedures) Act 1986 and local ethical approvals.

Slice Preparation. For electrophysiological experiments, rats ($n = 5$) were euthanized with sodium pentobarbital and transcardially perfused with ice-cold and oxygenated (95%O₂/5%CO₂) "slicing" solution containing (in mM) sucrose (214), KCl (2.0), NaH₂PO₄ (1.2), NaHCO₃ (26), MgSO₄ (1.3), CaCl₂ (2.4), D-glucose (10). Following decapitation, the brain was extracted and the meninges was gently removed. The brain was blocked and glued to a vibratome (Campden Instruments, Loughborough, Leics., UK), where 250 μ m-thick coronal slices of the hypothalamus containing SCN were prepared. Slices were immediately transferred to "recording" artificial cerebrospinal fluid (aCSF) containing (in mM) NaCl (127), KCl (2.0), NaH₂PO₄ (1.2), NaHCO₃ (26), MgCl₂ (1.3), CaCl₂ (2.4), and D-glucose (10) in a continuously oxygenated holding chamber at 35 °C for a period of 25 min. Subsequently, slices were allowed to recover in "recording" solution at room temperature for a minimum of 1 h before recording.

Whole-Cell Patch Clamp Recordings. For whole-cell recordings, slices were transferred to a submerged chamber and placed on an elevated grid that allows perfusion both above and below the slice. An Olympus BX-51 WI upright microscope (Olympus, Southend-on-Sea, Essex, UK) was used for infrared—differential interference contrast visualization of cells.

Recordings were performed at room temperature (22 °C) and slices were continuously perfused with oxygenated "recording" solution (as above) at a rate of ca. 5 mL/min, unless otherwise described. All pharmacological compounds were dissolved in "recording" solution and bath applied. Recording solution containing 1 μ M MCS-0382 was exposed to blue light (405 nm, 2.37 mW/mm²) for 10 min prior to application.

Whole cell current- and voltage-clamp recordings were performed with pipettes (3–7 M Ω when filled with intracellular solution) made from borosilicate glass capillaries (World Precision Instruments, Hitchin, Herts, UK) pulled on a P-97 Flaming/Brown micropipette puller (Sutter, Novato, CA, USA). The intracellular recording solution contained (in mM) K-gluconate (140), KCl (10), HEPES (10), EGTA (1), Na₂ATP (2), pH 7.3 (with KOH). Recordings were performed using a Multiclamp 700B amplifier and pClamp11 software (Molecular Devices, San Jose, CA, USA). Slow and fast capacitative

components were automatically compensated for. Access resistance was monitored throughout the experiments, and neurons in which the series resistance was >25 M Ω or changed >15% were excluded from the statistics. Liquid junction potential was 16.4 mV and not compensated. The recorded current was sampled at 10 kHz and filtered at 2 kHz unless otherwise stated.

Data and Statistical Analysis. The data and statistical analysis comply with the recommendations on experimental design and analysis in pharmacology,⁴⁹ using GraphPad Prism software. Data are presented as means \pm SEM of n independent experiments, performed at least in duplicates to ensure the reliability of single values. IC_{50} , EC_{50} and E_{max} values were obtained following non-linear regression (curve fit) with four parameters of data from a minimum of eight different concentrations per experiment, repeated at least three times independently. All assays performed here were previously validated and demonstrated the robustness and variability of the procedure using this number of independent experiments for concentration–response curves. When possible, data were normalized to maximal and minimum responses using melatonin response as a reference in order to avoid unwanted sources of variations, as differences in the amplitude of the melatonin effect between independent experiments.

■ ASSOCIATED CONTENT

SI Supporting Information

The Supporting Information is available free of charge at <https://pubs.acs.org/doi/10.1021/acs.jmedchem.2c00717>.

Additional photochemical and pharmacological data and compound characterization spectra (NMR and HPLC-MS) (PDF)

Molecular formula strings (CSV) (CSV)

■ AUTHOR INFORMATION

Corresponding Authors

Ralf Jockers – *Université de Paris, Institut Cochin, INSERM, CNRS, F-75014 Paris, France*; orcid.org/0000-0002-4354-1750; Email: ralf.jockers@inserm.fr

Amadeu Llebaria – *MCS, Laboratory of Medicinal Chemistry & Synthesis, Department of Biological Chemistry, Institute for Advanced Chemistry of Catalonia (IQAC-CSIC), 08034 Barcelona, Spain*; orcid.org/0000-0002-8200-4827; Email: amadeu.llebaria@iqac.csic.es

Authors

Gloria Somalo-Barranco – *Université de Paris, Institut Cochin, INSERM, CNRS, F-75014 Paris, France*; MCS, *Laboratory of Medicinal Chemistry & Synthesis, Department of Biological Chemistry, Institute for Advanced Chemistry of Catalonia (IQAC-CSIC), 08034 Barcelona, Spain*

Carme Serra – *MCS, Laboratory of Medicinal Chemistry & Synthesis, Department of Biological Chemistry, Institute for Advanced Chemistry of Catalonia (IQAC-CSIC), 08034 Barcelona, Spain*; SIMChem, *Synthesis of High Added Value Molecules, Institute of Advanced Chemistry of Catalonia (IQAC-CSIC), 08034 Barcelona, Spain*

David Lyons – *School of Physiology, Pharmacology and Neuroscience, Faculty of Life Sciences, University of Bristol, BS8 1TD Bristol, U.K.*

Hugh D. Piggins – *School of Physiology, Pharmacology and Neuroscience, Faculty of Life Sciences, University of Bristol, BS8 1TD Bristol, U.K.*

Complete contact information is available at:

<https://pubs.acs.org/10.1021/acs.jmedchem.2c00717>

Author Contributions

All authors have given approval to the final version of the manuscript. Conceptualization, A.L. and R.J.; chemical synthesis, G.S.-B. and C.S.; biochemical investigations, G.S.-B. and D.L.; supervision, H.D.P., A.L., and R.J.; writing—original draft, review, and editing, G.S.-B., A.L., and R.J.; funding acquisition, R.J., A.L., D.L., and H.D.P. designed the electrophysiological studies and D.L. carried out the recordings and analyzed the whole-cell recordings.

Notes

The authors declare no competing financial interest.

ACKNOWLEDGMENTS

This work was supported by Agence Nationale de la Recherche (ANR-19-CE16-0025-01 mitoGPCR to R.J.), Institut National de la Santé et de la Recherche Médicale (INSERM), Centre National de la Recherche Scientifique (CNRS) and by Ministerio de Ciencia e Innovación (MCIN), Agencia Estatal de Investigación (AEI), and ERDF-FEDER European Fund (projects CTQ2017-89222-R and PID2020-120499RB-I00) funded by MCIN/AEI/10.13039/501100011033 and by “ERDF A way of making Europe” by the European Union, and by the Catalan government (2017SGR1064). R.J. was supported by the Fondation de la Recherche Médicale (Equipe FRM DEQ20130326503), and ANR-21-CE18-00XX «alloGLP1R» and La Ligue Contre le Cancer N/Ref: RS19/75–127. G.S.B. was supported by a doctoral fellowship from the Fondation de la Recherche Médicale (FRM grant number ECO20170637544) obtained by R.J. D.L. and H.D.P. were supported by funds from the University of Bristol and a project grant from the Biotechnology and Biological Sciences Research Council UK (BBSRC grant number BB/R019223). We thank Lourdes Muñoz and Carolina Cera (SimChem, IQAC-CSIC, Barcelona) for support in the synthesis and analysis of compounds.

ABBREVIATIONS

DAD, diode array detector; DEAC, diethylaminocoumarin; DMAP, 4-dimethylaminopyridine; DMNB, 4,5-dimethoxy-2-nitrobenzyl; FBS, fetal bovine serum; GPCR, G protein-coupled receptor; *o*-NB, *o*-nitrobenzyl; PDA, photodiode array detector; PPG, photocleavable-protecting group; SAR, structure–activity relationship; SCN, suprachiasmatic nucleus; SEM, standard error of the mean; UV–vis, ultraviolet–visible

REFERENCES

- (1) Dubocovich, M. L.; Delagrange, P.; Krause, D. N.; Sugden, D.; Cardinali, D. P.; Olcese, J. International Union of Basic and Clinical Pharmacology. LXXV. Nomenclature, Classification, and Pharmacology of G Protein-Coupled Melatonin Receptors. *Pharmacol. Rev.* **2010**, *62*, 343–380.
- (2) Liu, J.; Clough, S. J.; Hutchinson, A. J.; Adamah-Biassi, E. B.; Popovska-Gorevski, M.; Dubocovich, M. L. MT1 and MT2 Melatonin Receptors: A Therapeutic Perspective. *Annu. Rev. Pharmacol. Toxicol.* **2016**, *56*, 361–383.
- (3) Cecon, E.; Oishi, A.; Jockers, R. Melatonin Receptors: Molecular Pharmacology and Signalling in the Context of System Bias. *Br. J. Pharmacol.* **2018**, *175*, 3263–3280.
- (4) Welleman, I. M.; Hoorens, M. W. H.; Feringa, B. L.; Boersma, H. H.; Szymański, W. Photoresponsive Molecular Tools for Emerging Applications of Light in Medicine. *Chem. Sci.* **2020**, *11*, 11672–11691.
- (5) Gorostiza, P.; Isacoff, E. Y. Optical Switches for Remote and Noninvasive Control of Cell Signaling. *Science* **2008**, *322*, 395–399.

- (6) Szymański, W.; Beierle, J. M.; Kistemaker, H. A. V.; Velema, W. A.; Feringa, B. L. Reversible Photocontrol of Biological Systems by the Incorporation of Molecular Photoswitches. *Chem. Rev.* **2013**, *113*, 6114–6178.
- (7) Ellis-Davies, G. C. R. Caged Compounds: Photorelease Technology for Control of Cellular Chemistry and Physiology. *Nat. Methods* **2007**, *4*, 619–628.
- (8) Ricart-Ortega, M.; Font, J.; Llebaria, A. GPCR photopharmacology. *Mol. Cell. Endocrinol.* **2019**, *488*, 36–51.
- (9) Berizzi, A. E.; Goudet, C. Strategies and Considerations of G-Protein-Coupled Receptor Photopharmacology. *Adv. Pharmacol.* **2020**, *88*, 143–172.
- (10) Gienger, M.; Hübner, H.; Löber, S.; König, B.; Gmeiner, P. Structure-Based Development of Caged Dopamine D2/D3 Receptor Antagonists. *Sci. Rep.* **2020**, *10*, 829.
- (11) Hansen, M. J.; Velema, W. A.; Lerch, M. M.; Szymanski, W.; Feringa, B. L. Wavelength-Selective Cleavage of Photoprotecting Groups: Strategies and Applications in Dynamic Systems. *Chem. Soc. Rev.* **2015**, *44*, 3358–3377.
- (12) Comai, S.; Gobbi, G. Unveiling the Role of Melatonin MT2 Receptors in Sleep, Anxiety and Other Neuropsychiatric Diseases: A Novel Target in Psychopharmacology. *J. Psychiatry Neurosci.* **2014**, *39*, 6–21.
- (13) Posa, L.; De Gregorio, D.; Gobbi, G.; Comai, S. Targeting Melatonin MT2 Receptors: A Novel Pharmacological Avenue for Inflammatory and Neuropathic Pain. *Curr. Med. Chem.* **2018**, *25*, 3866–3882.
- (14) Karamitri, A.; Jockers, R. Melatonin in Type 2 Diabetes Mellitus and Obesity. *Nat. Rev. Endocrinol.* **2019**, *15*, 105–125.
- (15) Nerbonne, J. M. Caged Compounds: Tools for Illuminating Neuronal Responses and Connections. *Curr. Opin. Neurobiol.* **1996**, *6*, 379–386.
- (16) Zlotos, D. P.; Jockers, R.; Cecon, E.; Rivara, S.; Witt-Enderby, P. A. MT1 and MT2 Melatonin Receptors: Ligands, Models, Oligomers, and Therapeutic Potential. *J. Med. Chem.* **2014**, *57*, 3161–3185.
- (17) Jockers, R.; Delagrange, P.; Dubocovich, M. L.; Markus, R. P.; Renault, N.; Tosini, G.; Cecon, E.; Zlotos, D. P. Update on Melatonin Receptors: IUPHAR Review 20. *Br. J. Pharmacol.* **2016**, *173*, 2702–2725.
- (18) Liu, L.; Jockers, R. Structure-Based Virtual Screening Accelerates GPCR Drug Discovery. *Trends Pharmacol. Sci.* **2020**, *41*, 382–384.
- (19) Elisi, G. M.; Scalvini, L.; Lodola, A.; Bedini, A.; Spadoni, G.; Rivara, S. In silico drug discovery of melatonin receptor ligands with therapeutic potential. *Expert Opin. Drug Discovery* **2022**, *17*, 343–354.
- (20) Bourbon, P.; Peng, Q.; Ferraudi, G.; Stauffacher, C.; Wiest, O.; Helquist, P. Synthesis, Photophysical, Photochemical, and Computational Studies of Coumarin-Labeled Nicotinamide Derivatives. *J. Org. Chem.* **2012**, *77*, 2756–2762.
- (21) Salah, F.; Purohit, V.; Ferraudi, G.; Stauffacher, C.; Wiest, O.; Helquist, P. PHP-Tethered N-Acyl Carbamate: A Photocage for Nicotinamide. *Org. Lett.* **2018**, *20*, 2547–2550.
- (22) Bourbon, P.; Peng, Q.; Ferraudi, G.; Stauffacher, C.; Wiest, O.; Helquist, P. Development of Carbamate-Tethered Coumarins as Phototriggers for Caged Nicotinamide. *Bioorg. Med. Chem. Lett.* **2013**, *23*, 6321–6324.
- (23) Zhang, W.; Lohman, A. W.; Zhuravlova, Y.; Lu, X.; Wiens, M. D.; Hoi, H.; Yaganoglu, S.; Mohr, M. A.; Kitova, E. N.; Klassen, J. S.; Pantazis, P.; Thompson, R. J.; Campbell, R. E. Optogenetic Control with a Photocleavable Protein, Phocl. *Nat. Methods* **2017**, *14*, 391–394.
- (24) Mizuno, H.; Mal, T. K.; Tong, K. I.; Ando, R.; Furuta, T.; Ikura, M.; Miyawaki, A. Photo-Induced Peptide Cleavage in the Green-to-Red Conversion of a Fluorescent Protein. *Mol. Cell* **2003**, *12*, 1051–1058.
- (25) Lira-Rocha, A.; Espejo-González, O.; Naranjo-Rodríguez, E. B. Receptor-Binding Studies of 1-N-Substituted Melatonin Analogues. *Eur. J. Med. Chem.* **2002**, *37*, 945–951.

- (26) Journé, A. S.; Habib, S. A. M.; Dodda, B. R.; Morcos, M. N. F.; Sadek, M. S.; Tadros, S. A. A.; Witt-Enderby, P. A.; Jockers, R.; Zlotos, D. P. N1-Linked Melatonin Dimers as Bivalent Ligands Targeting Dimeric Melatonin Receptors. *Medchemcomm* **2014**, *5*, 792–796.
- (27) Viault, G.; Poupart, S.; Mourlevat, S.; Lagaraine, C.; Devavry, S.; Lefoulon, F.; Bozon, V.; Dufourny, L.; Delagrangé, P.; Guillaumet, G.; Suzenet, F. Design, Synthesis and Biological Evaluation of Fluorescent Ligands for MT1 and/or MT2 Melatonin Receptors. *RSC Adv.* **2016**, *6*, 62508–62521.
- (28) Voelker, T.; Ewell, T.; Joo, J.; Edstrom, E. D. O-Nitrobenzyl as a Photocleavable Nitrogen Protecting Group for Indoles, Benzimidazole, and 6-Chlorouracil. *Tetrahedron Lett.* **1998**, *39*, 359–362.
- (29) Wendell, C. I.; Boyd, M. J. Reevaluation of the 2-Nitrobenzyl Protecting Group for Nitrogen Containing Compounds: An Application of Flow Photochemistry. *Tetrahedron Lett.* **2015**, *56*, 897–899.
- (30) Macor, J. E.; Cuff, A.; Cornelius, L. Neutral Acylation (Protection) of the Indole Nitrogen: A Simple Synthesis of Indole-1-Carboxylates, Indole-1-Thiocarboxylates and Indole-1-Carboxamides. *Tetrahedron Lett.* **1999**, *40*, 2733–2736.
- (31) Schaper, K.; Etinski, M.; Fleig, T. Theoretical Investigation of the Excited States of 2-Nitrobenzyl and 4,5-Methylenedioxy-2-Nitrobenzyl Caging Groups. *Photochem. Photobiol.* **2009**, *85*, 1075–1081.
- (32) Schade, B.; Hagen, V.; Schmidt, R.; Herbrich, R.; Krause, E.; Eckardt, T.; Bendig, J. Deactivation Behavior and Excited-State Properties of (Coumarin-4-Yl)methyl Derivatives. I. Photocleavage of (7-Methoxycoumarin-4-Yl)methyl-Caged Acids with Fluorescence Enhancement. *J. Org. Chem.* **1999**, *64*, 9109–9117.
- (33) Kohl-Landgraf, J.; Buhr, F.; Lefrançois, D.; Mewes, J. M.; Schwalbe, H.; Dreuw, A.; Wachtveitl, J. Mechanism of the Photoinduced Uncaging Reaction of Puromycin Protected by a 6-Nitroveratryloxycarbonyl Group. *J. Am. Chem. Soc.* **2014**, *136*, 3430–3438.
- (34) Martinez, G. R.; Almeida, E. A.; Klitzke, C. F.; Onuki, J.; Prado, F. M.; Medeiros, M. H. G.; Di Mascio, P. Measurement of Melatonin and Its Metabolites: Importance for the Evaluation of Their Biological Roles. *Endocrine* **2005**, *27*, 111–118.
- (35) Ferry, G.; Ubeaud, C.; Lambert, P. H.; Bertin, S.; Cogé, F.; Chomar, P.; Delagrangé, P.; Serkiz, B.; Bouchet, J. P.; Truscott, R. J. W.; Boutin, J. A. Molecular Evidence That Melatonin Is Enzymatically Oxidized in a Different Manner than Tryptophan: Investigations with Both Indoleamine 2,3-Dioxygenase and Myeloperoxidase. *Biochem. J.* **2005**, *388*, 205–215.
- (36) Bonnefont-Rousselot, D.; Collin, F.; Jore, D.; Gardès-Albert, M. Reaction Mechanism of Melatonin Oxidation by Reactive Oxygen Species in Vitro. *J. Pineal Res.* **2011**, *50*, 328–335.
- (37) van den Top, M.; Buijs, R. M.; Ruijter, J. M.; Delagrangé, P.; Spanswick, D.; Hermes, M. L. H. J. Melatonin Generates an Outward Potassium Current in Rat Suprachiasmatic Nucleus Neurons in Vitro Independent of Their Circadian Rhythm. *Neuroscience* **2001**, *107*, 99–108.
- (38) Jiang, Z. G.; Nelson, C. S.; Allen, C. N. Melatonin Activates an Outward Current and Inhibits Ih in Rat Suprachiasmatic Nucleus Neurons. *Brain Res.* **1995**, *687*, 125–132.
- (39) Scott, F. F.; Belle, M. D. C.; Delagrangé, P.; Piggins, H. D. Electrophysiological Effects of Melatonin on Mouse Per1 and Non-Per1 Suprachiasmatic Nuclei Neurons in Vitro. *J. Neuroendocrinol.* **2010**, *22*, 1148–1156.
- (40) Gobbi, G.; Comai, S. Differential Function of Melatonin MT1 and MT2 Receptors in REM and NREM Sleep. *Front. Endocrinol.* **2019**, *10*, 87.
- (41) Feng, S.; Harayama, T.; Montessuit, S.; David, F. P. A.; Winssinger, N.; Martinou, J. C.; Riezman, H. Mitochondria-Specific Photoactivation to Monitor Local Sphingosine Metabolism and Function. *Elife* **2018**, *7*, No. e34555.
- (42) Farley, S.; Laguerre, A.; Schultz, C. Caged Lipids for Subcellular Manipulation. *Curr. Opin. Chem. Biol.* **2021**, *65*, 42–48.
- (43) Suofu, Y.; Li, W.; Jean-Alphonse, F. G.; Jia, J.; Khattar, N. K.; Li, J.; Baranov, S. V.; Leronna, D.; Mihalik, A. C.; He, Y.; Cecon, E.; Wehbi, V. L.; Kim, J. H.; Heath, B. E.; Baranova, O. V.; Wang, X.; Gable, M. J.; Kretz, E. S.; Di Benedetto, G.; Lezon, T. R.; Ferrando, L. M.; Larkin, T. M.; Sullivan, M.; Yablonska, S.; Wang, J.; Minnigh, M. B.; Guillaumet, G.; Suzenet, F.; Richardson, R. M.; Poloyac, S. M.; Stolz, D. B.; Jockers, R.; Witt-Enderby, P. A.; Carlisle, D. L.; Vilaradaga, J. P.; Friedlander, R. M. Dual Role of Mitochondria in Producing Melatonin and Driving GPCR Signaling to Block Cytochrome c Release. *Proc. Natl. Acad. Sci. U.S.A.* **2017**, *114*, E7997–E8006.
- (44) Gbahou, F.; Cecon, E.; Viault, G.; Gerbier, R.; Jean-Alphonse, F.; Karamitri, A.; Guillaumet, G.; Delagrangé, P.; Friedlander, R. M.; Vilaradaga, J. P.; Suzenet, F.; Jockers, R. Design and Validation of the First Cell-Impermeant Melatonin Receptor Agonist. *Br. J. Pharmacol.* **2017**, *174*, 2409–2421.
- (45) Jockers, R.; Da Silva, A.; Strosberg, A. D.; Bouvier, M.; Marullo, S. New Molecular and Structural Determinants Involved in β 2-Adrenergic Receptor Desensitization and Sequestration. *J. Biol. Chem.* **1996**, *271*, 9355–9362.
- (46) Work, T. S.; Work, E. Chapter 2: Methods of Cell Breakage: Assessing Their Suitability and Efficacy. *Lab. Tech. Biochem. Mol. Biol.* **1979**, *7*, 11–44.
- (47) Ayoub, M. A.; Levoe, A.; Delagrangé, P.; Jockers, R. Preferential Formation of MT1/MT2 Melatonin Receptor Heterodimers with Distinct Ligand Interaction Properties Compared with MT 2 Homodimers. *Mol. Pharmacol.* **2004**, *66*, 312–321.
- (48) Kamal, M.; Gbahou, F.; Guillaume, J. L.; Daulat, A. M.; Benleulmi-Chaachoua, A.; Luka, M.; Chen, P.; Kalbasi Anaraki, D. K.; Baroncini, M.; Mannoury la Cour, C. M.; Millan, M. J.; Prevot, V.; Delagrangé, P.; Jockers, R. Convergence of Melatonin and Serotonin (5-HT) Signaling at MT2/5-HT2C Receptor Heteromers. *J. Biol. Chem.* **2015**, *290*, 11537–11546.
- (49) Curtis, M. J.; Alexander, S.; Cirino, G.; Docherty, J. R.; George, C. H.; Giembycz, M. A.; Hoyer, D.; Insel, P. A.; Izzo, A. A.; Ji, Y.; MacEwan, D. J.; Sobey, C. G.; Stanford, S. C.; Teixeira, M. M.; Wonnacott, S.; Ahluwalia, A. Experimental Design and Analysis and Their Reporting II: Updated and Simplified Guidance for Authors and Peer Reviewers. *Br. J. Pharmacol.* **2018**, *175*, 987–993.
- (50) Josa-Culleré, L.; Llebaria, A. In the Search for Photocages Cleavable with Visible Light: An Overview of Recent Advances and Chemical Strategies. *ChemPhotoChem* **2021**, *5*, 296–314.
- (51) Sitkowska, K.; Hoes, M. F.; Lerch, M. M.; Lameijer, L. N.; van der Meer, P.; Szymański, W.; Feringa, B. L. Red-Light-Sensitive BODIPY Photoprotecting Groups for Amines and Their Biological Application in Controlling Heart Rhythm. *Chem. Commun.* **2020**, *56*, 5480–5483.